land

MDPI

Article

Projecting Water Yield Amidst Rapid Urbanization: A Case Study of the Taihu Lake Basin

Rui Zhou [1], Yanan Zhou [1,*], Weiwei Zhu [2,*], Li Feng [1] and Lumeng Liu [1]

[1] Key Laboratory of Soil and Water Processes in Watershed, College of Geography and Remote Sensing, Hohai University, Nanjing 211000, China; zhouhohai@hhu.edu.cn (R.Z.); fly@hhu.edu.cn (L.F.); liulumeng@hhu.edu.cn (L.L.)

[2] Key Laboratory of Remote Sensing and Digital Earth, Aerospace Information Research Institute, Chinese Academy of Sciences, Beijing 100101, China

* Correspondence: zhouyn@hhu.edu.cn (Y.Z.); zhuww@aircas.ac.cn (W.Z.)

Abstract: Changes in land cover and land use (LULC) can impact water availability by altering the structure and functioning of land ecosystems. Accurately projecting the impacts of LULC on water yield (WY) is of utmost importance for regional landscape management. Taking the rapidly urbanizing Taihu Lake Basin (TLB) as an example, coupled with the PLUS-InVEST model, three scenarios of a natural development (ND) scenario, urban development (UD) scenario, and ecological protection (EP) scenario were set to simulate the response mechanisms of land use changes for WY and the influence of policy-making on the water conservation capacity of river basins. (1) During 2000 and 2020, the Taihu Lake Basin (TLB) experienced rapid urbanization, which was evident in the conversion of forest and cropland for urban development. (2) From 2000 to 2020, the TLB's WY first decreased and then increased, ranging from 201.52 × 10^8 m^3 to 242.70 × 10^8 m^3. Spatially, an uneven distribution pattern of WY depth emerged, with mountainous and hilly regions exhibiting higher WY compared to plain areas. Temporally, changes in total WY were primarily influenced by precipitation, while areas with increased WY showed a certain correlation with regions experiencing an expansion of construction land. (3) By 2030, the TLB will continue to expand construction land under the UD scenario, while the area of ecological land will expand under the EP scenario. WY is expected to vary across scenarios, with the highest yield observed under the UD scenario, followed by the ND scenario, while the EP scenario exhibits the lowest yield. These findings can offer scientifically informed insights and guidance for future WY changes, carrying substantial effects for maintaining ecological preservation and promoting high-quality development in the TLB.

Keywords: water yield; multi-scenario simulation; PLUS; InVEST; Taihu Lake Basin

check for updates

Academic Editor: Shicheng Li

Received: 11 December 2024
Revised: 7 January 2025
Accepted: 7 January 2025
Published: 13 January 2025

Citation: Zhou, R.; Zhou, Y.; Zhu, W.; Feng, L.; Liu, L. Projecting Water Yield Amidst Rapid Urbanization: A Case Study of the Taihu Lake Basin. *Land* **2025**, *14*, 149. https://doi.org/10.3390/land14010149

Copyright: © 2025 by the authors. Licensee MDPI, Basel, Switzerland. This article is an open access article distributed under the terms and conditions of the Creative Commons Attribution (CC BY) license (https://creativecommons.org/licenses/by/4.0/).

1. Introduction

Ecosystem services benefit humans both directly and indirectly, serving as the fundamental basis for human well-being and prosperity [1,2]. The "Beautiful China 2035" plan was formally unveiled on 27 March 2023, with the objective of enhancing the functions of key ecosystem services and fostering sustainable growth in China. Ecosystem service assessments are important for evaluating the overall well-being of ecosystems, creating effective environmental regulations, and promoting sustainable development. Specifically, the increasing disparity between the availability of water and the demand for it, exacerbated by the effects of global climate change and population increase, has made the evaluation of water yield (WY) services essential for efficient water resource management [3,4]. As

a critical element of ecosystems, WY services, which provide essential water resources, play a key role in maintaining the balance and sustainability of the water cycle, preserving biodiversity and ecological stability, supporting agricultural production, and fulfilling drinking water requirements [5,6].

Numerous studies have concentrated on the exploration and application of ecosystem service assessment methods. Initially, researchers sought to introduce a model for quantifying the economic value of each unit of area, sparking interest in the assessment of ecosystem services [7]. According to the study conducted by [7], Xie, et al. [8] proposed the "China Ecosystem Service Equivalence Factor Table" in light of China's actual situation, and it has since gained widespread use. In recent years, with advancements in Earth observation technology and geographic information technology, numerous studies have primarily focused on developing various models for assessing ecosystem services, including the ARIES model [9], which utilizes multi-scale and multi-resolution data to quantify ecosystem services; the TESSA model [10], designed to facilitate rapid and cost-effective ecosystem service assessments in diverse settings; the SolVES model [11], known for its capacity to simulate ecosystem service dynamics over time; the EcoMetrix model [12], focusing on translating ecological data into economic values; and the InVEST (Integrated Valuation of Ecosystem Services and Trade-offs) model [13], a comprehensive tool that facilitates the analysis of trade-offs between ecosystem services and human well-being. Among these, the InVEST model has gained widespread application in dynamic assessments of ecosystem service functions due to its low data requirements, high evaluation accuracy, and unambiguous geographical expression of results [14]. However, previous studies of WY in the Taihu Lake Basin have primarily focused on quantitative estimations [15,16] or examining how the current LULC or climate impacts ecosystem services [17–19]. These studies have not included simulations under different scenarios, representing a gap in the current literature.

Regarding the WY services, the kinds and alterations of LULC directly influence the hydrological processes and WY of ecosystems, which in turn affect their general functioning and provision of services [20]. Different LULC activities, such as forestry, agriculture, and grasslands, significantly impact how precipitation is intercepted, infiltrated [21], and runs off due to their varying types of vegetation cover and soil characteristics. Thus, it is essential to investigate the impact of LULC changes on the WY of ecosystems. To catch the LULC changes and their WY services, many LULC simulation models are implemented, including the Automaton (CA) model [22,23] the Conversion of LULC and its Effects at Small regional extent (CLUE-S) model [24,25], the Multi-Agent System (MAS) model (Yuan et al., 2014), and the Future LULC Simulation (FLUS) model [26,27]. These prediction models have mostly concentrated on enhancing modeling approaches, rules, and precision, while paying less attention to the fundamental factors that drive LULC and its changes over time [28]. Recently, Liang, et al. [29] developed the PLUS model, integrating the Land Expansion Analysis Strategy (LEAS) and a Cellular Automaton model using multiple types of Random Seed Patches (CARS), which offers a comprehensive patch-level dynamic simulation and data mining capabilities for LULC. The PLUS model mimics patch-level variations in different LULC types more accurately and excavates the causes of LULC changes more thoroughly than previous models. In particular, adding LULC planning rules to the next multi-scenario simulation improves the realism and citation value of the findings [30].

Researchers have recently endeavored to integrate the PLUS model and the InVEST model in order to forecast and evaluate forthcoming LULC changes as well as ecosystem service functions. Sun, et al. [31] employed the InVEST and PLUS models to forecast carbon storage in Nanjing under various scenarios, concluding that policies aimed at protecting farms and ecology can successfully mitigate the decline in carbon storage. Wang, et al. [32]

conducted a simulation to study LULC changes and carbon storage in Chongqing. The findings indicated that the ecological conservation scenario yielded the most advantages for sustainable development and exhibited the highest anticipated carbon values. Hu, et al. [33] employed the PLUS-InVEST model to replicate the habitat quality in Baoding. Their research uncovered that the scenario focused on conserving farmland resulted in the best level of habitat quality. Chen, et al. [34] investigated the variations in WY within the Bosten Lake Basin, considering both temporal and spatial factors. They found that places with higher altitudes tended to have higher WY, while the lowest WY was observed under the ecological protection scenario.

While the PLUS model enhances the ability to predict changes in LULC, its integration with the InVEST model provides valuable assessments of ecosystem service values, together improving forecasts of geographical and temporal patterns. However, the utilization of these models to investigate future WY patterns on regional scales remains significantly underexplored. This notable gap highlights the pressing need for more extensive research that utilizes these models to better understand regional WY dynamics amidst evolving land use scenarios.

The Taihu Lake Basin (TLB) is located in the Yangtze River Delta Economic Zone in China. Over the past three decades, the TLB has experienced quick economic growth and significant LULC transformations, including urbanization and the expansion of agriculture [35]. Because of the significant role played by this region in food and industrial production, conflicts between humans and the land, as well as water scarcity, have become more noticeable. In order to resolve this matter, the Taihu Basin Authority of the Ministry of Water Resources issued the "Comprehensive Planning for the Taihu Basin (2012–2030)", aiming to achieve a basic balance between water resource supply and demand [36], ensuring comprehensive security of the basin's water supply, and achieving an urban and rural water supply guarantee rate of 95–97%. Thus, this study presents three scenarios—natural development, urban development, and ecological protection—combining the InVEST and PLUS models to predict future LULC patterns under multiple scenarios and evaluating the corresponding WY.

Within the scope of this research, we developed a comprehensive framework to evaluate the spatiotemporal patterns of WY under multiple future scenarios in the TLB. We employed the PLUS-based LULC simulation and the InVEST-based WY calculation to construct this framework. The detailed targets of this investigation are as follows: (1) identifying the spatiotemporal changes in LULC in the TLB from 2000 to 2020, (2) quantitatively assessing the WY of the TLB from 2000 to 2020 and the WY based on the different vegetation types and sub-basins, and (3) predicting the WY under multiple scenarios of LULC changes in 2030.

The ensuing portions of the paper are organized as follows: Section 2 presents the study area, datasets and the details of the method. In Section 3, experiments were carried out to examine the spatiotemporal changes in LULC and the WY variation characteristics in the TLB. Section 4 concludes this paper with several major conclusions.

2. Materials and Methods

2.1. Study Area

The Taihu Lake Basin (Figure 1), situated in the eastern region of the Yangtze River Delta in China, spans from 30° to 32.5° N latitude and 119° to 122° E longitude. It covers an area of 36,895 km^2 and stretches across 3 provinces and 1 municipality, including Anhui, Jiangsu, Zhejiang, and Shanghai. The TLB has a relatively flat topography that mainly consists of mountains, hills, and plains, and the elevation above sea level ranges from 0 to 1500 m. Mountains and hills are generally located in the west, while the plains cover

around 80% of the entire area of the basin [37]. The TLB is in the subtropical monsoon climate zone, which is characterized by annual temperature ranging from 15 to 17 °C and an annual precipitation of 1000 to 1400 mm. The precipitation is primarily concentrated in spring and summer. These environmental conditions result in a distinct hydrological system in the mountainous upstream parts and a river network in the downstream plain areas [38]. Its water resource zoning can be categorized into four regions: the western and lake areas, Wuyang District, Hangjiahu District, and Huangpu River District. Each year, it provides more than 2.1 billion cubic meters of tap water to Jiangsu, Zhejiang, and Shanghai.

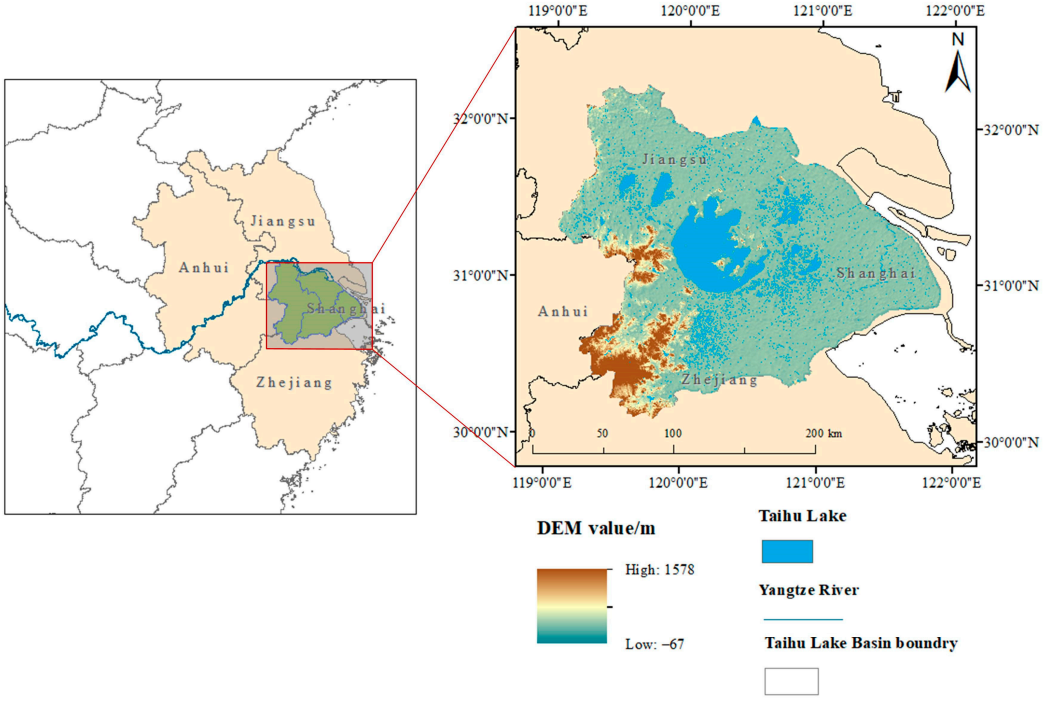

Figure 1. Geographical location and water distribution of the TLB.

According to the 2023 Water Resources Bulletin of the Taihu Basin and Southeast Rivers issued by the Taihu Basin Management Bureau, the total population of the TLB is 68.59 million, accounting for 4.9% of the country's total population. As one of the most economically developed and socially vibrant regions, the TLB is of significance in China. Although the TLB only covers 0.4% of China's territory, it contributes 9.8% of the national GDP, and the per capita GDP is 181,000 yuan, 2.2 times higher than the national average [39].

Quantitative evaluations of the WY in the ecosystem can provide a solid scientific basis and aid in decision-making for the advancement of ecological civilization in the basin.

2.2. Datasets and Preprocessing

Multisource datasets (Table 1) were collected to assess the spatiotemporal patterns of WY in the TLB using the InVEST (3.14.1) and PLUS (v1.40) models. The datasets of InVEST included precipitation, evapotranspiration, LULC data, digital elevation data, and soil physical and chemical property data. For the PLUS model, the dataset included precipitation, elevation, slope, GDP, population, and road data as input variables.

The LULC data were selected from three time periods: 2000, 2010, and 2020. The research area's characteristics led to the reclassification of 17 data categories into six distinct types: cropland, forest, grassland, water, construction land, and unused land (includes bare areas, consolidated bare areas, and unconsolidated bare areas).

Table 1. Datasets for evaluating the spatiotemporal patterns of WY in the TLB.

Data Type	Data Name	Data Resolution	Data Source
LULC Data	LULC Data	30 m	https://data.casearth.cn/ (acecessed on 6 March 2023)
Socioeconomic Data	Distance to Railways/Roads	1 km	https://www.openstreetmap.org/ (acecessed on 24 March 2023)
	Population	1 km	https://www.resdc.cn/ (acecessed on 24 March 2023)
	GDP	1 km	https://www.resdc.cn/
Climate Data	DEM	1 km	http://www.gscloud.cn (acecessed on 24 March 2023)
	Slope and Aspect Data	1 km	Generated from DEM
	Soil Physicochemical Properties	1 km	http://globalchange.bnu.edu.cn/ (acecessed on 6 March 2023)
	Annual Evapotranspiration	1 km	https://portal.casearth.cn/ (acecessed on 6 March 2023)
	Annual Average Precipitation	1 km	https://portal.casearth.cn/
	Annual Average Temperature	1 km	https://portal.casearth.cn/

The soil physical and chemical dataset includes nationwide data on soil thickness, soil density, soil structure, and organic matter.

The estimation of the available water content for vegetation is accomplished by the utilization of a nonlinear fitting model that relies on soil texture and soil organic matter [40]. For generating the WY raster map, the soil depth for water bodies (reservoirs and rivers) and artificial impervious surfaces (settlements) is set to zero, replacing the maximum rooting depth of vegetation.

The required precipitation data for the model use the average values for the three years before and after the years 2000, 2010, and 2020 under the corresponding LULC conditions.

The InVEST model requires the vegetation evapotranspiration coefficient to adjust the reference evapotranspiration and obtain potential evapotranspiration. This coefficient can be obtained from relevant research results or by consulting data from the United Nations Food and Agriculture Organization. The Zhang coefficient, representing the characteristics of precipitation, is an experimental constant that varies between 1 and 30. Based on the natural geographical characteristics of the TLB, we set its value to 6.5, as referenced from the related literature [41]. To ensure consistency in the spatial data accuracy, raster data are cropped and resampled to 30 m × 30 m in the WGS_1984_UTM_Zone50N coordinate system.

2.3. Methods

This study utilized an encompassing framework to evaluate the spatiotemporal patterns of WY under multiple future scenarios in the TLB through the combined use of the PLUS-based LULC simulation and the InVEST-based WY calculation (Figure 2). The framework consists of three main steps, including (1) data selection and processing; (2) the calculation of WY under multiple future scenarios combining the InVEST model and the PLUS model; and (3) a quantitative analysis of spatiotemporal fluctuations in WY and LULC. Firstly, integrating climate and LULC data, the InVEST model quantified the WY of the TLB spanning from 2000 to 2020. Secondly, using natural and social factors as variables, the PLUS model predicted LULC under different scenarios in 2030. Finally, the LULC data acquired from the PLUS model were utilized as input and integrated with the InVEST model to compute WY in several scenarios for the year 2030, further identifying how WY and LULC change over time and space in the TLB.

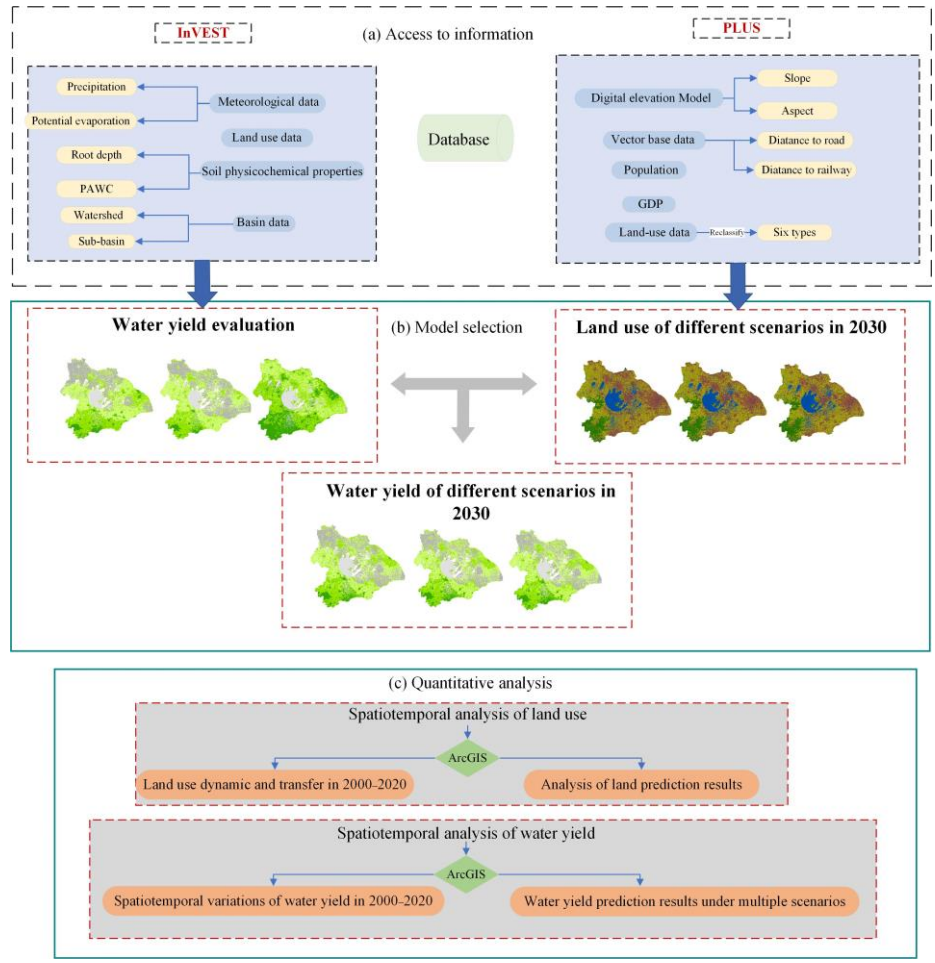

Figure 2. Flowchart for evaluating the spatiotemporal patterns of WY under multiple future scenarios in the TLB.

2.3.1. Water Yield Calculation Using InVEST

The InVEST water yield model (hereafter referred to as InVEST model) [42] was chosen to compute the WY in the TLB, since it can leverage geographic information systems and offer advantages in spatial analysis and visualization [43]. The WY calculation predominantly depends on the Budyko theory and the concept of water balance. The InVEST model utilizes raster data for its operation, considering only the WY of individual grid cells without computing WY between cells. It calculates the water produced by various LULC types (grid units) within a watershed, aggregating the results for the entire watershed and its sub-watersheds. Both surface runoff and groundwater recharge are considered ecosystem WY, thus ignoring temporal and spatial transformations between water on the surface and underground. Consequently, the WY is derived by subtracting evapotranspiration from precipitation [44].

The InVEST model requires input raster data such as the soil depth, annual average precipitation, soil available water content, annual potential evapotranspiration, and LULC, along with watershed and sub-watershed vector data. Biophysical coefficient tables (maximum root depth and vegetation transpiration coefficients for various LULC types) and a seasonal constant Z are set to complete the data input, followed by running the model to obtain results. The InVEST calculates WY for different LULC cells using the following formula:

$$Y_{xj} = \left(1 - AET_{xj}/P_x\right) \cdot P_x \quad (1)$$

$$AET_{xj}/P_x = 1 + R_{xj} - \left[1 + \left(R_{xj}\right)^w\right]^{1/w} \quad (2)$$

$$\omega_x = Z \cdot AWC_x/P_x \quad (3)$$

$$R_{xj} = k_{xj} \cdot ETo_x/P_x \quad (4)$$

In the formula, Y_{xj} represents the WY for LULC type j at grid cell x; AET_{xj} is the actual annual evapotranspiration for LULC type j at grid cell x; P_x is the annual precipitation at grid cell x; ω_x is a dimensionless parameter; R_{xj} is the Budyko dryness index for LULC type j at grid cell x; Z is the Zhang coefficient, indicating parameters for rainfall distribution and depth; AWC_x is the available water capacity of the soil at grid cell x; k_{xj} is the vegetation evapotranspiration coefficient for land cover type j at grid cell x; and ETo_x is the potential evapotranspiration at grid cell x.

2.3.2. Future LULC Simulation Using PLUS

The PLUS simulates future LULC changes by integrating LULC type data and employing LULC Expansion Analysis Strategy (LEAS) within a Cellular Automaton (CA) model driven by multiple random patch seeds [29]. This model requires the input of LULC data from two different time periods. By overlaying the analysis, dynamic elements of LULC changes during the evolution process are obtained and presented in raster data format. The model employs the random forest technique to determine the correlations between LULC types and potential drivers, establishing reliable mathematical models to reveal patterns of change. Consequently, potential transition probabilities and development trends of LULC conversions are derived, and corresponding pixel patches are generated based on the parameters.

2.3.3. LULC Scenario Simulation and Threshold Setting

Several factors exert effects on the future growth of urban areas and changes in LULC. Therefore, when simulating and predicting urban LULC changes, it is essential to consider various environmental factors. The "Comprehensive Plan of the Taihu Lake Basin" issued by the Ministry of Water Resources [36] pointed out the significance of safeguarding wetland and lake ecosystems, aiming to improve the watershed's ecological service functions by implementing ecological restoration initiatives. Additionally, it suggests enforcing the ecological red line system strictly, limiting the strain of urban expansion on the environment, and preventing development and encroachment on environmentally vulnerable areas. In this study, we use it as a guiding document and develop three scenarios: the natural development (ND) scenario, urban development (UD) scenario, and ecological protection (EP) scenario.

ND: This scenario disregards the impact of planning policies on LULC changes, extending the 2010–2020 LULC patterns with constant transition probabilities between land types. Using a 10-year interval, Markov chains predict the LULC demand for 2030 in the TLB under natural growth.

UD: In this situation, the likelihood of transforming cropland, forest, and grassland into construction land rises by 20% relatively, while the likelihood of transforming construction land into other categories (except cropland) is relatively reduced by 30%. Based on the ND predictions, it forecasts the 2030 LULC demand under the urban protection priority.

EP: The possibility of transforming forest and grassland into construction land is relatively reduced by 50%, the likelihood of turning cropland into construction land decreases by 30%, and the transformation of construction land to forest relatively increases by 10%. Habitat degradation is strictly prohibited, with regional water bodies as constraints. It predicts the 2030 LULC demand under ecological protection.

The LULC demand refers to the number of grid cells for different LULC types in the simulated years. It mainly includes two simulation methods: linear regression and Markov chain. This study employed the Markov chain method to forecast the quantity of grid cells for each LULC type in the year 2030. The calculation results are shown in Table 2 and Figure 3.

Table 2. Land demands (km^2).

LULC	Cropland	Forest	Grassland	Water Bodies	Construction Land	Unused Land
2020	18,135.9	3855.8	188.1	4816.1	9569.7	8.8
2030ND	16,531.0	3748.4	212.0	4900.7	11,172.8	9.4
2030UD	16,118.8	3740.7	204.3	4880.0	11,621.3	9.3
2030EP	17,563.3	3766.8	218.9	4924.4	10,091.5	9.5

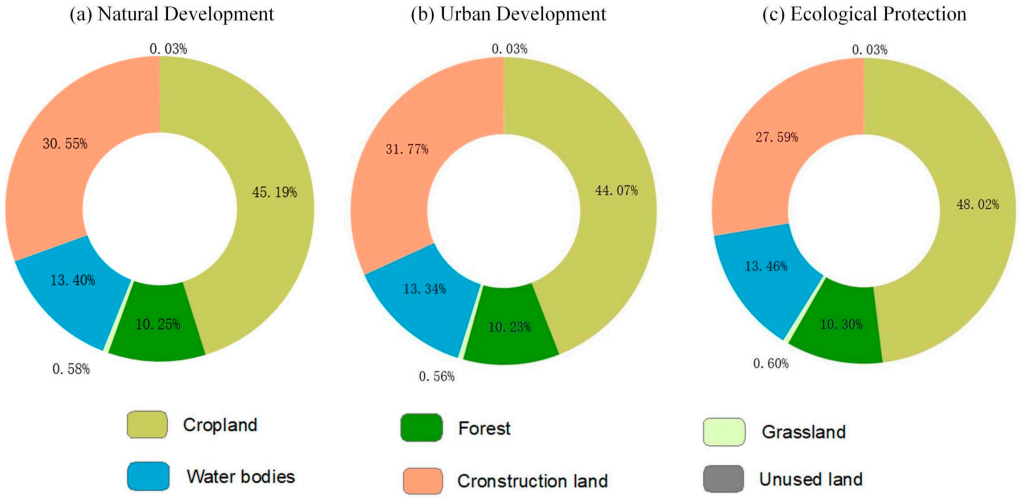

Figure 3. The proportions of land use types under three future scenarios.

The neighborhood weight indicates the expansion capability of different LULC types. In this study, the neighborhood weights were determined using the dimensionless ΔTA values from 2010 to 2020 (Table 3). The calculation formula is as follows:

$$w_i = (\Delta TA_i - \Delta TA_{min})/(\Delta TA_{max} - \Delta TA_{min}) \quad (5)$$

Table 3. Neighborhood weights of each variety according to ΔTA.

Variety	Cropland	Forest	Grassland	Water Bodies	Construction Land	Unused Land
ΔTA	−2,254,105	−112,567	44,512	136,556	2,184,696	908
weight	0	0.4824	0.5178	0.5385	1	0.5080

In the equation, ΔTA_i represents the change in expansion area for each land cover type; ΔTA_{min} represents the minimum change in expansion area for each land cover type; and ΔTA_{max} represents the maximum change in expansion area for each land cover type.

The transition matrix represents the conversion rules between different LULC types. Specifically, when one LULC type cannot be converted to another, the corresponding value in the matrix is 0; otherwise, it is 1. The LULC change rules designed for multiple scenarios in this study are illustrated in Table 4.

Table 4. Transfer matrix.

	ND Scenario						UD Scenario						EP Scenario					
	A	**B**	**C**	**D**	**E**	**F**	**A**	**B**	**C**	**D**	**E**	**F**	**A**	**B**	**C**	**D**	**E**	**F**
A	1	1	1	1	1	1	1	0	0	0	1	1	1	1	1	1	1	1
B	1	1	1	1	1	1	1	1	1	0	1	1	1	0	1	0	0	0
C	1	1	1	1	1	1	1	1	1	1	1	1	1	0	1	1	0	0
D	0	0	0	1	0	0	0	0	0	1	1	0	0	0	0	0	1	0
E	0	0	0	0	1	0	0	0	0	0	1	0	0	0	0	0	1	0
F	1	1	1	1	1	1	1	1	1	1	1	1	1	1	1	1	1	1

Note: A. cropland, B. forest, C. grass, D. water bodies, E. construction land, F. unused land. Zero means that conversion to another land type is prohibited, and 1 means that conversion to another land type is allowed.

3. Results and Analysis

3.1. Spatiotemporal Analysis of LULC

3.1.1. Dynamic Changes in LULC

The predominant LULC types in the TLB are cropland and construction land (Figure 4). Cropland and construction land are extensively distributed across all regions except the southwestern hilly area, serving as the primary areas of human activity. Other areas mainly consist of forest and grassland, with forest occupying a significant proportion. In 2020, the LULC composition of the TLB was as follows: cropland (49.58%), construction land (26.16%), water bodies (13.16%), forest (10.54%), grassland (0.51%), and unused land (0.02%). The growth of construction land has resulted in a substantial reduction in the amount of cropland, while changes in forest and water bodies have been relatively minor. Unused land and construction land have shown evident expansion trends.

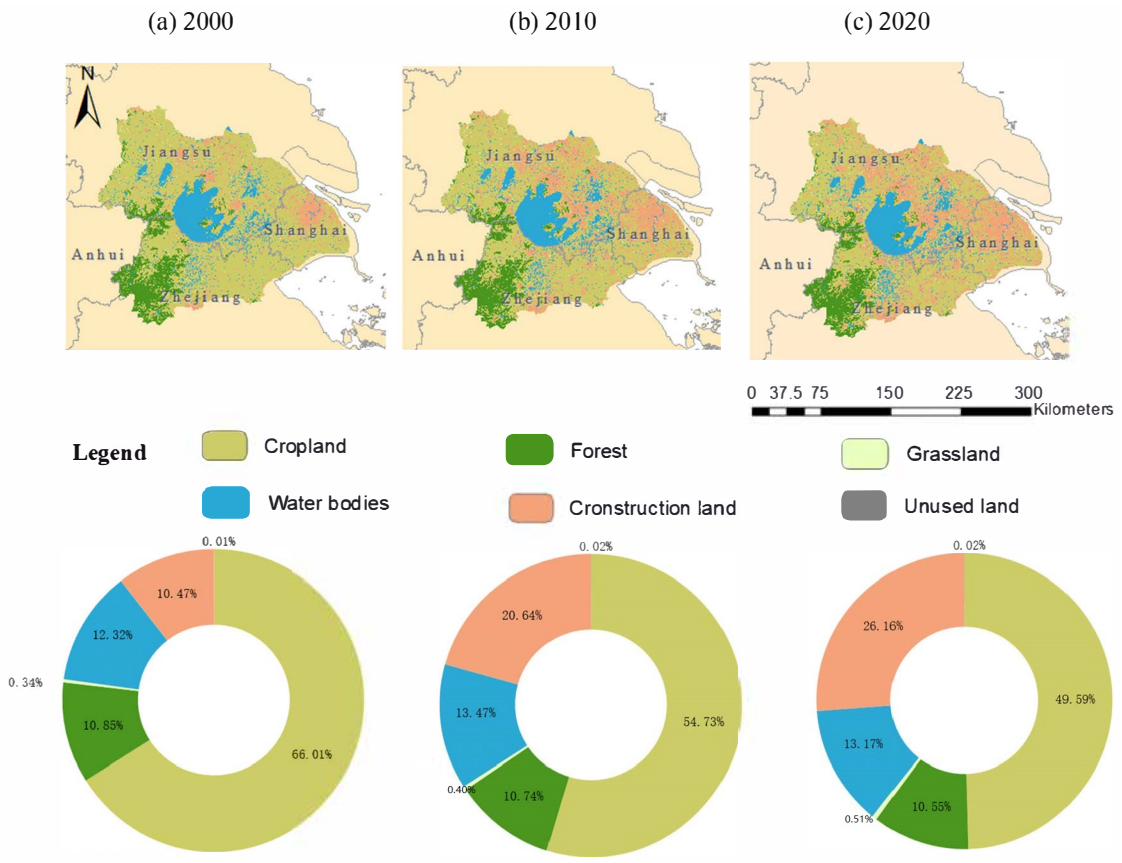

Figure 4. Changes in LULC types in the TLB from 2000 to 2020.

Table 5 indicates the average annual change over the 10-year period. During the period from 2000 to 2010, the dynamicity of all LULC types was relatively high, indicating rapid LULC changes. Construction land experienced the highest growth rate, with an annual change rate of 9.8%, totaling an increase of 3773 km^2 and reflecting the accelerated urbanization process during this period. Cropland experienced the most significant decrease, with an annual change rate of −1.65%. From 2010 to 2020, the annual change rate of LULC types relatively slowed down, possibly due to the implementation of national policies regulating construction land and protecting basic cropland. Construction land continued to expand, but at a slower pace, indicating the effectiveness of government control measures. The increase rate of grassland gradually rose, which was possibly associated with returning farmland to grassland and construction along the lakeshore. Changes in water bodies remained relatively stable, with slow changes in the water area that were likely related to basin water diversion projects. During the period from 2010 to 2020, the grassland area increased, reaching its peak growth rate of 2.7% and adding 39.99 km^2. The dynamicity of forests showed slow changes from 2000 to 2020, while unused land experienced rapid expansion from 2000 to 2010, increasing by 5.2 km^2.

Table 5. Average annual change in LULC over the 10-year period.

Study Period	Cropland		Forest		Grassland	
	Change Area (km^2)	Change %	Change Area (km^2)	Change %	Change Area (km^2)	Change %
2000–2010	−3980	−1.65%	−9.0	−0.02%	24.79	2.01%
2010–2020	−2029	−1.01%	−100.5	−0.25%	39.99	2.70%
Study Period	**Water bodies**		**Construction land**		**Unused land**	
	Change Area (km^2)	Change %	Change Area (km^2)	Change %	Change Area (km^2)	Change %
2000–2010	456.5	1.01%	3773	9.80%	5.2	18.48%
2010–2020	−147.8	−0.30%	1966	2.60%	0.8	1.00%

3.1.2. Transition Analysis of LULC

The total area of the TLB is 36,578 km^2. The rapid and intensive process of urbanization has resulted in substantial alterations in LULC types between the years 2000 and 2020. The land transition Sankey diagram (Figure 5) illustrates that the transitions are primarily dominated by cropland and construction land. From 2000 to 2010, significant acreage of unused land was transformed into construction areas. From 2010 to 2020, some areas previously converted from cropland to non-agricultural uses reverted to agricultural production, indicating a partial recovery of cropland. However, a large portion was still converted to other land use types. Construction land continued to increase, though the growth rate slowed.

Between 2000 and 2020, the most significant change in the TLB was the conversion of 6008.8 km^2 of land to construction areas, accompanied by a loss of 6844.1 km^2 of cropland.

Approximately 9.5% of the basin's grassland and 24% of its cropland were converted into construction land, resulting in a significant expansion of the construction land area. This trend suggests that urbanization accelerated during this period, driven by the significant expansion of construction land, which was fueled by the prevailing urbanization and industrialization trends. The TLB was in a period of rapid economic development, with urban areas rapidly expanding into surrounding areas, resulting in a 150% increase in construction land area primarily at the cost of cropland. There was an increase in the grassland area from 123 km^2 in 2000 to 188 km^2 in 2020, representing a rise from 0.34% to 0.51% of the basin. The total inflow of water bodies was 309 km^2, showing an increasing

trend. The overall change in forest was relatively small, with a total outflow of 239.8 km^2 over the 20-year period. Another significant change during this period was the conversion of 12.29% of unused land into cropland, grassland, and forest, leading to the development of previously unused land. In summary, human activities have had the greatest impact on cropland and construction land in the TLB over the past two decades, with varying degrees of impact on forest, grassland, and water bodies.

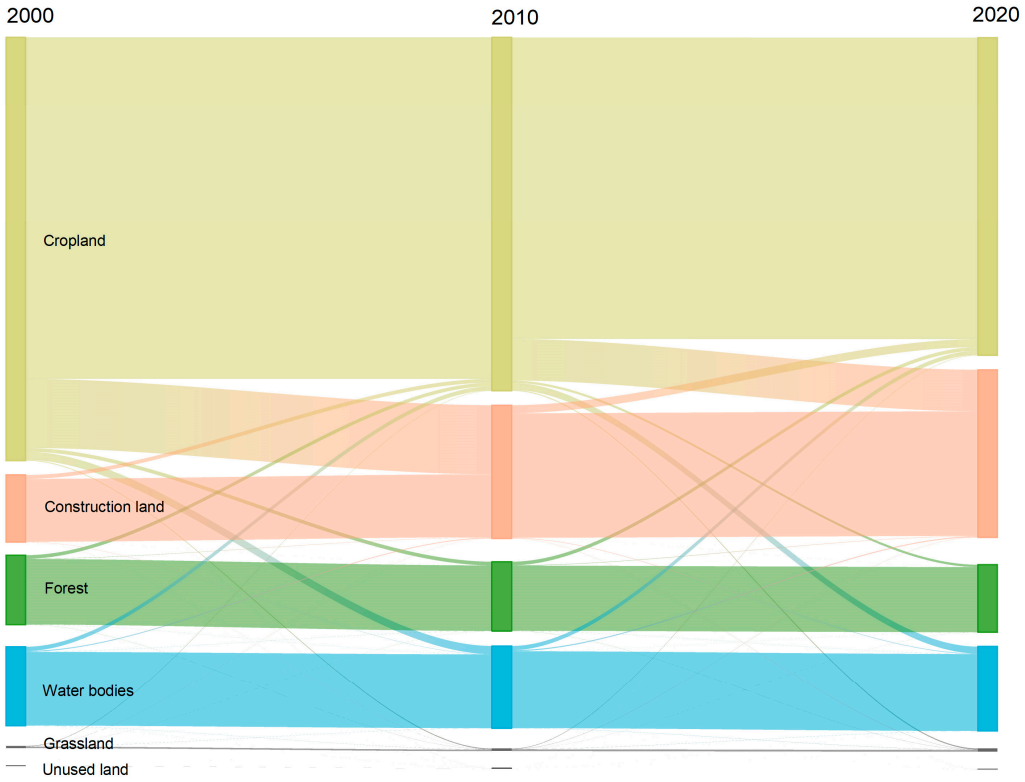

Figure 5. LULC transfer Sankey map for 2000—2020 (km^2).

3.1.3. Analysis of the Land Prediction Results

To evaluate whether the model's simulation accuracy meets the research objectives, the LULC data from 2010 and 2015 were used as the baseline. Using the 2010 LULC data as the reference, the computed transition probabilities were applied to the PLUS model to predict the simulated LULC for 2020. The comparison results presented in Figure 6 and Table 6 show that the simulation accuracy is high, with minimal discrepancies from the observed values. The overall accuracy is 0.9522, and the Kappa coefficient is 0.9268, indicating a high level of reliability in predicting LULC changes. This suggests that the model fulfills the requirements for further study.

Table 6. Comparison of real and simulated LULC patterns in 2020.

LULC (2020)	Cropland	Forest	Grassland	Water Bodies	Construction Land	Unused Land
Actual proportion	50.24%	10.56%	0.50%	13.13%	25.55%	0.02%
Simulated proportion	49.59%	10.54%	0.51%	13.17%	26.16%	0.02%

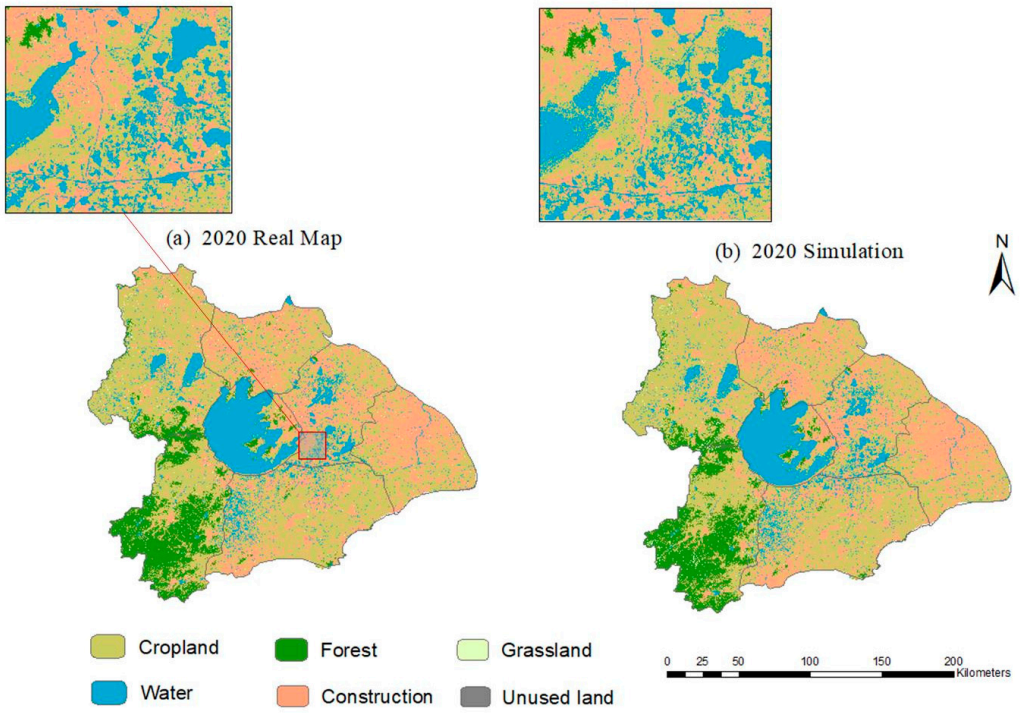

Figure 6. Comparison of the 2020 forecasted results and actual situation.

According to the LULC type maps of different scenarios in 2030 obtained through the PLUS model (Table 7), the LULC distribution maps (Figure 7) and the area and change rate of LULC types under different scenarios for 2030 are derived as follows:

Table 7. The area of LULC under various 2030 scenarios and its change from 2020 (km^2).

Year		Development Scenario	Cropland	Forest	Grassland	Water	Construction	Unused Land
Area	2020	-	18,135.9	3855.8	188.1	4816.1	9569.7	8.8
	2030	ND	16,531.0	3754.0	212.0	4900.6	11,172.8	7.4
		UD	16,118.8	3793.6	204.3	4832.4	11,621.3	7.5
		EP	17,563.3	3865.6	181.8	4868.7	10,091.5	7.0
Total percent change		ND	−8.86%	−2.68%	12.77%	1.76%	16.75%	−16.11%
		UD	−11.13%	−1.66%	8.67%	0.34%	21.43%	−14.77%
		EP	−3.17%	0.21%	−3.29%	1.10%	5.45%	−20.84%

ND—By 2030, the LULC change trends for various land classes are generally consistent with those from 2010 to 2020. Compared with the LULC data for 2020, under the ND scenario, the size of construction land, water bodies, and grassland will expand by 16.75%, 1.76%, and 12.77%, respectively, as shown in Table 7. Of them, the unused land will have the greatest drop, with a reduction rate of 8.86%. The forests, on the other hand, would fall by 2.68%, mostly in hilly regions. Although the forests have had a consistent decline in size over time, they are still able to sustain a portion of more than 10%. The unused land area will shrink by 16.11%, suggesting that a significant portion of the idle land has been developed.

UD—With the acceleration of urbanization, a large amount of cropland is gradually being replaced by urban construction, with the amount of cropland reduced by 2017.6 km^2 compared to 2020. Construction land has expanded sharply, increasing by 21.43%. Industrial parks and commercial centers in the urban fringe areas continue to expand. Compared to the natural scenario, the forest area further decreases, while the growth rates of grassland and water bodies both decline, indicating a significant shift in the LULC structure.

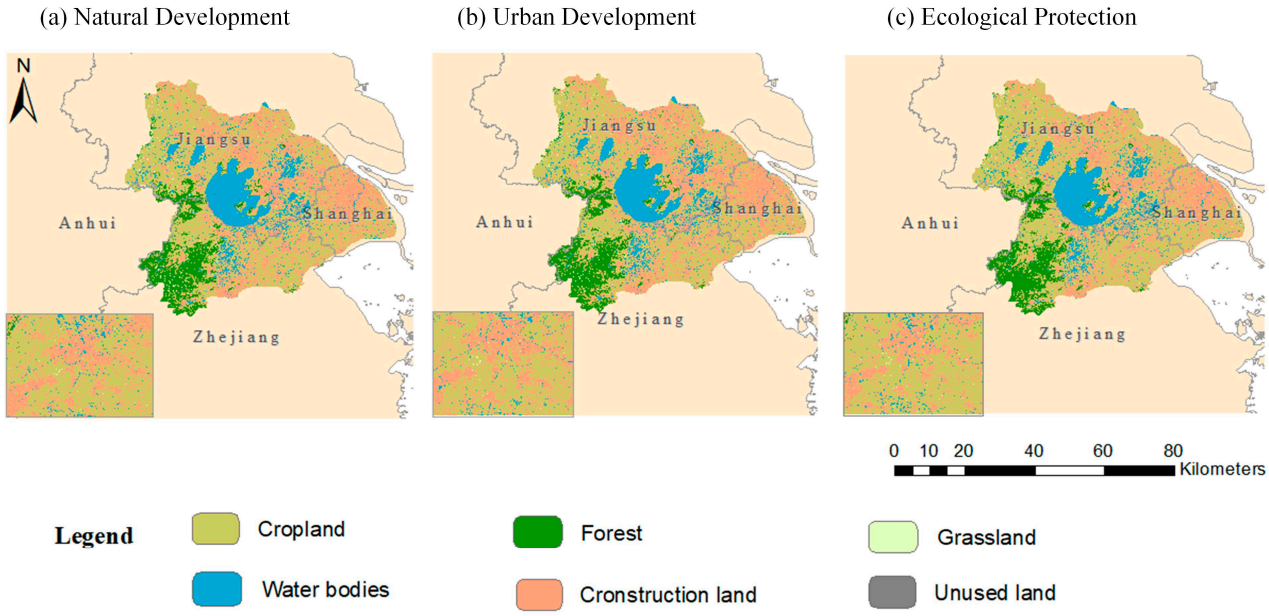

Figure 7. LULC changes in the TLB in 2030 under different scenarios.

EP—In this situation, actions have been taken to safeguard agriculture, forest, and grassland, resulting in a significant reduction in the growth rate of construction land to 5.45%. The rate of cropland reduction has likewise experienced a substantial decline, reaching a mere 3.17%. In this scenario, the area of water bodies is observed to rise by 52.59 km^2, while the forest area experiences a growth of 111.6 km^2. The successful implementation of ecological protection and restoration measures, as specified in the "Action Plan for Advancing the New Round of Comprehensive Treatment of Taihu Lake" by the Jiangsu Provincial Government, can be credited for the positive outcomes. These measures include enhancing ecological protection and restoration efforts, establishing protective forests along the lake, and making adjustments to aquaculture layouts.

3.2. Analysis of Water Yield Variation Characteristics in the TLB

3.2.1. Analysis of Spatiotemporal Variations in WY

The spatial differentiation pattern of WY depth in different periods in the TLB exhibits relatively small differences, demonstrating an overall consistent regularity (Figure 8). Generally, WY increases from the northeast to the southwest. Mountainous and hilly areas exhibit a relatively higher WY compared to plain areas.

Comparing 2020 with 2000, the per unit area ecosystem WY depth in most areas increased (Table 8). In 2000, the WY in the TLB was 209.2 $\times$ 10^8 m^3, with a per unit area ecosystem WY depth ranging from 0 to 1167 mm and an average of 572 mm. In 2010, the WY was 201.5 $\times$ 10^8 m^3, with a per unit area ecosystem WY depth ranging from 0 to 1119 mm and an average of 551 mm. In 2020, the WY was 242.7 $\times$ 10^8 m^3, with a per unit area ecosystem WY depth ranging from 0 to 1276 mm and an average of 663 mm. From 2000 to 2020, the annual average precipitation in the basin showed a trend of first decreasing and then increasing.

The areas with high WY are mainly concentrated in the southwestern part of the watershed, specifically in the Lake West area, where the average rainfall is significantly higher than in other areas of the TLB. There are large areas of bamboo forests and tea plantations in this region, and high vegetation cover also promotes transpiration, which contributes to precipitation formation. Additionally, the region's steep terrain leads to a prominent water collection effect, and the significant interception effect of forest on rainfall to some extent affects the total WY. Although impervious surfaces in each sub-region have

continuously increased with the urbanization process, this region still maintains a terrain pattern dominated by mountains and hills, which to some extent limits the increase in WY in the Lake West region. Conversely, the WY in the western and northern parts of the basin, such as the Wu Yang District, is relatively weak: the rainfall in this area is at a lower level than the rest of the basin, thereby making it difficult to effectively accumulate water resources. Low WY areas are mainly distributed in the western part of the lake and the lake area itself. In some areas in the northwest, rice is the main crop, resulting in large areas of paddy soil. Paddy soil is typically rich in organic matter, fine in texture, and has good water retention properties, reducing surface runoff.

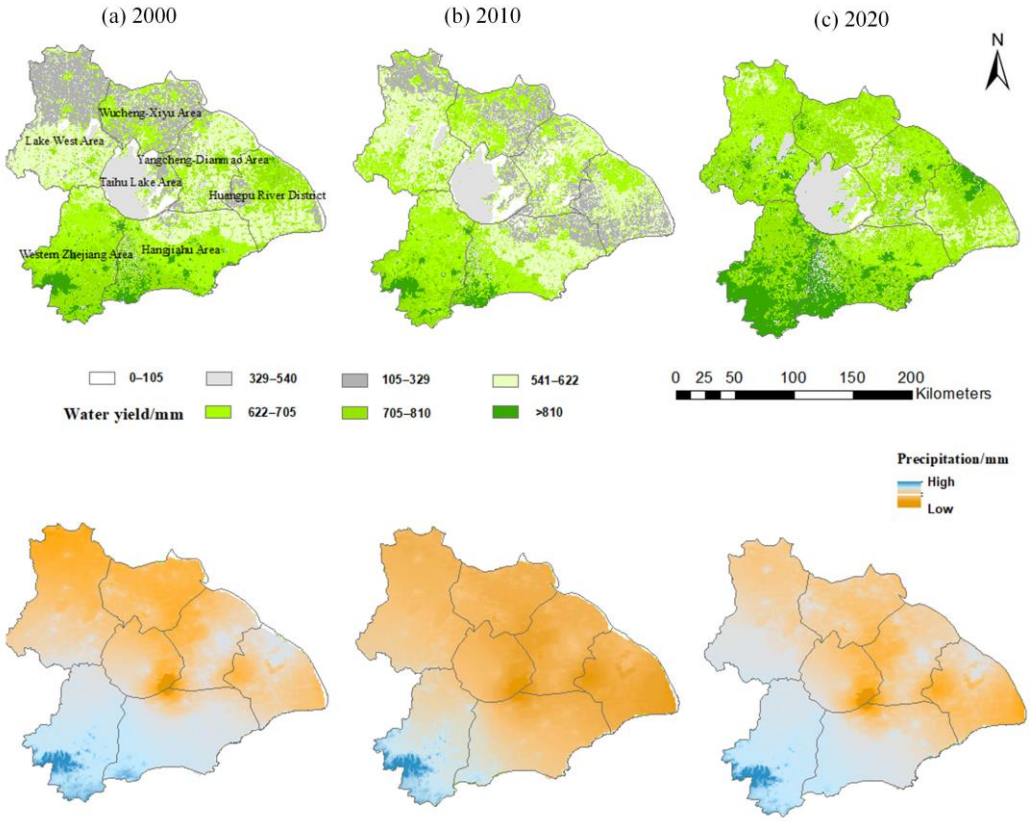

Figure 8. Water yield and the precipitation in the TLB from 2000 to 2020.

Table 8. WY and Precipitation in Various Zones of the TLB from 2000 to 2020.

Area	Total WY/10^8 m^3			Precipitation/mm		
Year	**2000**	**2010**	**2020**	**2000**	**2010**	**2020**
Lake West and Lake Area	91.25	93.04	110.35	963.0	977.2	1087.6
Wuyang District	43.43	42.15	51.42	884.1	870.6	992.0
Hangjiahu District	46.49	41.72	50.43	1019.2	951.6	1079.5
Huangpu River District	28.09	24.61	30.48	1019.2	841.0	975.0
Total	209.27	201.52	242.70	963.5	932.2	1051.3

The WY in 2010 decreased compared to 2000, which is a comprehensive reflection of the direct impacts of climate factors and LULC factors. Due to the reduction in precipitation and the rise in average annual temperature (approximately 0.05 °C per year), the evapotranspiration rate in the watershed continuously increased. The evaporation from construction land was limited only by atmospheric conditions and was more sensitive to rising temperatures during the study period, which is one of the factors contributing to the decline in WY compared to the year 2000.

From 2000–2020, Table 8 demonstrates that changes in precipitation were the primary driver of changes in total WY. During this period, urbanization in the eastern plain region accelerated, with built-up areas rapidly expanding around central cities and major transportation corridors. This expansion led to a significant increase in the proportion of impermeable surfaces in these areas. In regions where precipitation also increased, areas with higher densities of construction land tended to experience a shift in WY from lower to higher values, showing more pronounced changes compared to other land use types. For instance, in Huangpu District, WY still increased in 2020 despite a slight decrease in precipitation compared to 2000. This illustrates that rapid urbanization significantly altered the regional LULC patterns, which was also one of the factors contributing to the increase in WY.

3.2.2. Water Yield of Different LULC Types

Based on the principles of the InVEST model, the WY of a grid cell is primarily influenced by precipitation and evapotranspiration. Due to varying evapotranspiration capacities across different land use types and differences in litter water retention and canopy interception among these categories, changes in land use directly impact water production [20]. To compare the WY efficiency of different land use types under the same precipitation conditions and to eliminate the impact of precipitation on WY, we divided the total WY of each land use type by the total precipitation, yielding the WY efficiency for each land use type.

As illustrated in Figure 9, the WY across different LULC types is inversely proportional to the vegetation evapotranspiration on that land type. Compared to other LULC types, construction land, which lacks vegetation interception, shows lower evapotranspiration and thus higher WY depths. Conversely, water bodies, which are characterized by intense evaporation, exhibit lower WY depths.

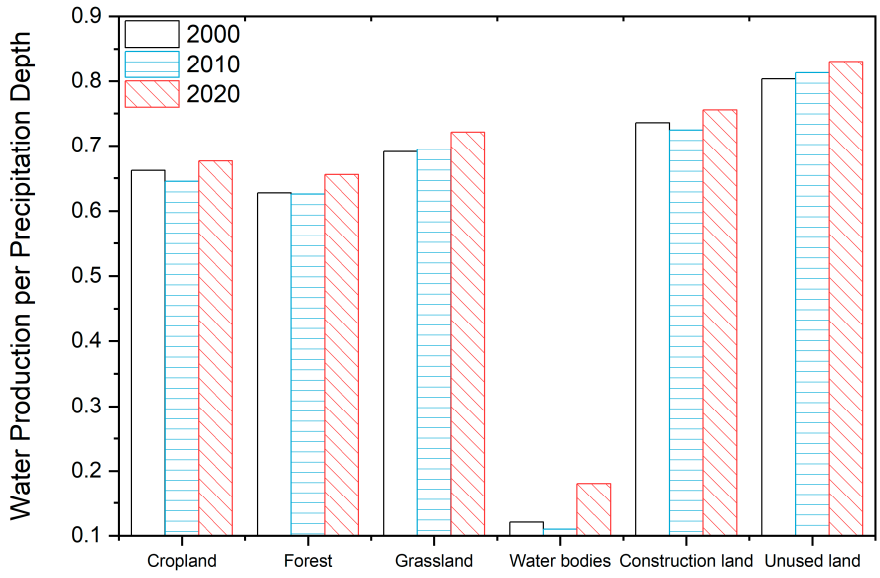

Figure 9. WY depths of different LULC types.

Construction and unused lands exhibit higher WY and are primarily located in the eastern plains of the basin where precipitation is abundant, vegetation cover is sparse, actual evapotranspiration is lower than other land cover types, and the infiltration of precipitation is hindered, resulting in higher WY depths. Compared to impervious surfaces and unused land, grasslands allow the partial infiltration of precipitation, and cropland in the basin, often composed of paddy soil, typically has a high organic content and good

soil structure, which helps retain more water, thereby reducing the WY depth. Areas with high vegetation cover, such as grasslands, exhibit a strong evapotranspiration capacity, resulting in lower WY depths compared to impervious surfaces and unused land with weaker evapotranspiration capacity. Forest areas, primarily composed of deciduous trees and situated in the southwest hills, exhibit a lower WY compared to cropland and grassland. The forest litter enriches the soil with organic matter, improving its water retention capacity. Furthermore, the deep root systems of these trees extract water from deeper soil layers and exhibit high evapotranspiration rates, which reduce surface and shallow soil water levels, ultimately contributing to a decrease in WY. Water bodies exhibit pronounced seasonal and interannual variability in WY, with a weaker water supply capacity due to the strong evapotranspiration capacity inherent to aquatic ecological land. This demonstrates that under constant conditions, an increase in construction land leads to an increased WY, while an increase in forest land reduces WY.

3.2.3. Analysis of WY Prediction Results Under Multiple Scenarios

Assuming that the multi-year average evapotranspiration and precipitation in the study area remain consistent with those of 2020, simulations of WY in the TLB for the year 2030 were conducted. Utilizing the PLUS model to process LULC data in conjunction with the InVEST model, predictions of WY for three scenarios in 2030 were obtained (Figure 10). Spatially, under different scenarios, the UD exhibits the widest coverage of high-value WY areas while the EP scenario results in the lowest WY among the three scenarios.

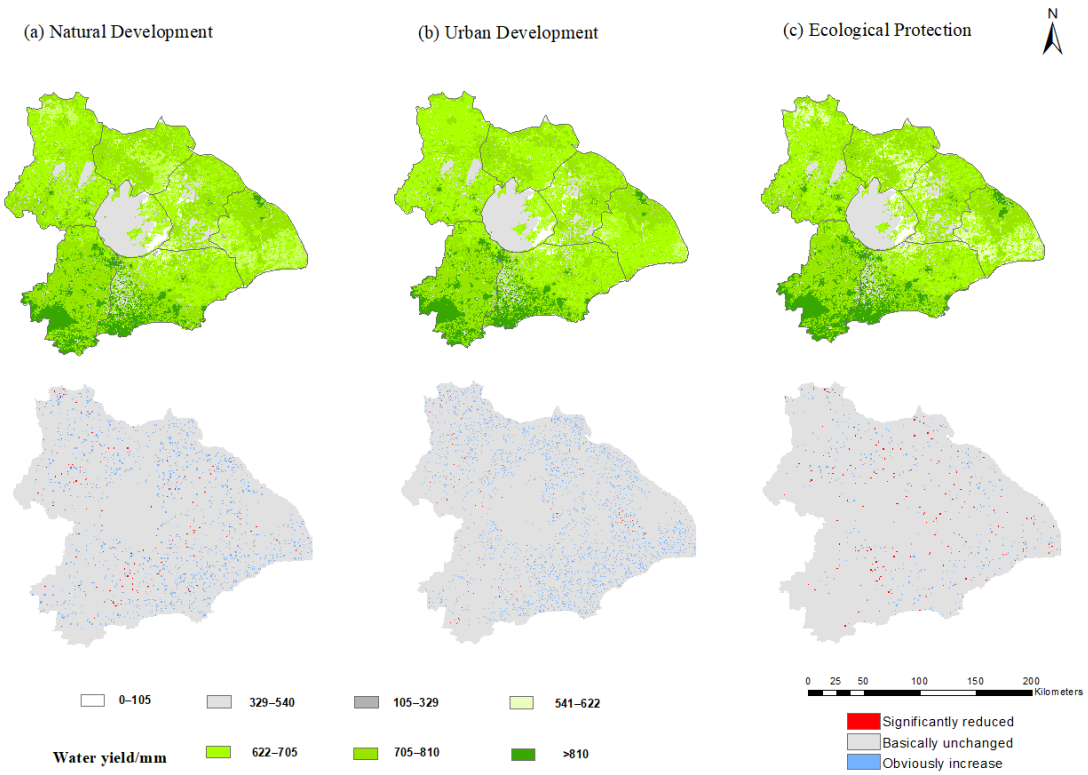

Figure 10. WY changes in the TLB under different scenarios.

In the ND scenario, the WY is 245.2 $\times$ 10^8 m^3, most areas continue to show an upward trend in WY, and the regions with increased WY correspond closely with areas of expanded construction land. During this scenario, the basin maintains the rapid urbanization and cropland degradation trends observed from 2000 to 2020, leading to a decreased soil water retention capacity in certain areas and thereby increasing the surface WY. Urbanization, by removing forests and other green vegetation, reduces plant transpiration and canopy

interception, significantly lowering total evapotranspiration and infiltration, and thus substantially increasing surface runoff.

In the UD scenario, the WY is 248.6 $\times$ 10^8 m^3, areas with increased WY are more densely distributed, and red areas with increased WY further decrease, especially in regions that are already urbanized or are urbanizing rapidly. In this scenario, as urban development leads to the transformation of cropland, forests, and grasslands into construction lands, the area covered by impervious surfaces increases, thereby increasing surface runoff. Spatially, the areas with an increased WY depth are primarily concentrated around existing urbanized regions.

In the EP scenario, the water yield is 243.4 $\times$ 10^8 m^3, regions with significantly increased WY are relatively few, and the blue areas representing unchanged conditions are notably reduced. In this scenario, the expansion of urban construction land is effectively controlled, the degradation rate of cropland slows, and forest areas, for the first time, shift from decline to growth. The increases in forests and grasslands enhance the soil water retention capacity and strengthen the interception of surface runoff, effectively mitigating the increase in WY depth in mountainous areas and reducing the risk of soil erosion. Additionally, protective measures for water bodies lead to an increase in WY in regions like Huzhou and Suzhou. Therefore, the implementation of scientific measures for grassland and forest conservation can effectively curb the increase in WY, contributing to the protection of water sources, conservation of biodiversity, and sustainable use of soil and water resources, while potentially mitigating flood risks in certain contexts.

4. Discussion

Compared to some existing studies of WY [45], this research goes further by predicting WY under LULC changes. Changes in LULC types affect WY by modifying soil types and textures and altering the structure of the underlying surface. These alterations influence the dynamics of both surface and groundwater systems, thereby impacting WY [46].

4.1. Effects of Land Use Changes on Water Yield

From 2000 to 2020, significant changes in LULC were observed, with cropland and built-up areas being the most prominent [47]. The expansion of construction land that encroaches on agricultural land, particularly in hilly and urban areas, will persist as a significant characteristic of future LULC changes without intervention. The formation of and changes in LULC are significantly influenced by policies and regulations, directly affecting future developments. In accordance with the goals and specifications outlined in the "Comprehensive Planning for the Taihu Basin (2012–2030)", we have produced UD and EP scenarios. The study discovered that various policy orientations and development goals have substantial influences on LULC, as well as the trends of LULC transformation. More precisely, the simulation of the LULC in 2030 showed that cropland and construction land exhibit a more pronounced response to these policy changes, which is similar to the finding in the Upper Bhima River Basin [48].

The results indicate a trend of increasing WY from the northeast to the southwest in the TLB. The mountainous and hilly areas in the southwest exhibit a relatively higher WY compared to the plains, influenced by a combination of LULC and climate. In the past 20 years, the temporal and spatial variations in WY have been significant, with an uneven distribution and differences in WY depth across various LULC types. These findings are consistent with results from other basins and regions, such as the Yellow River Basin [49], Ebinur Lake Basin [50], Sancha River Basin [51], Xitiaoxi River Basin [52], and Luo River Basin [53]. Wang [54] studied WY depths for different LULC types on Hainan Island and

found that built-up areas had the highest unit area WY depth, followed by orchards, with water bodies having the lowest, similar to the results of this study.

The evaluation of the 2030 LULC simulation for the TLB reveals an increase in WY across all three scenarios. Among them, the UD scenario exhibits the highest WY, while the EP scenario shows the lowest WY. From a methodological perspective, the water yield module of the InVEST model is based on the Budyko water–heat coupling balance assumption, in which evapotranspiration is considered as water loss. In general, precipitation is strongly correlated with actual evapotranspiration and potential evapotranspiration, which can be regarded as direct driving factors of WY. This study investigates the dynamic changes in ecosystem WY in three planning scenarios under the given climatic conditions, and the relative changes in WY in 2030 between three scenarios reach 5.2×10^8 m^3. In the EP scenario, WY significantly decreases compared to the other two scenarios, with the highest WY observed under the UD scenario. The spatial growth pattern of construction land coincides with the areas exhibiting significant increases in WY, suggesting that socio-economic factors and urbanization also influence WY.

The application of the PLUS model helps optimize the LULC and its structure, thereby resolving the conflict between the utilization of land resources in a watershed and the growth of socio-economic factors. Tao, et al. [55] found that urbanization and land use have strong effects on hydrologic services at the sub-basin scale, similar to the conclusions of our study. Although these factors are not direct drivers, their influences are indirect, and the alignment of construction land growth with regions showing increased WY is consistent with findings from other studies [17,25,56].

4.2. Advantages and the Constraints of the Model Used in This Research

The influence of policies and regulations on LULC is closely linked to the direction of LULC changes over time. However, past studies just investigated the individual effects of climate change and LULC changes on WY, and there is a shortage of comprehensive investigations of the collective impacts of LULC changes on WY across multiple scenarios. This study, based on the "Comprehensive Planning for the Taihu Basin (2012–2030)", establishes limitations for UD and EP. The utilization of a scenario-based research method allows for the simulation and evaluation of WY under various scenarios, enhancing our understanding of how changes in LULC can potentially affect WY. The PLUS model is superior to previous models for simulating LULC changes. It has the ability to dynamically model the geographical and temporal changes in various LULC patches, resulting in more precise simulation outcomes [57].

While the InVEST model is well-established and highly applicable in China, this study's omission of the upstream water supply to the region might lead to overestimated InVEST results. The seasonal factor Z value was set to 6.5, which may introduce some errors due to small watershed climate factors. The model localization and lack of long-term field observation data could affect the accuracy of the research results. Future research should enhance field data monitoring, adjust the model parameters for localization, and ensure the reliability of the evaluation's results.

Apart from ND, only UD and EP were included, which might not fully represent the diversity of real-life scenarios. Developing additional scenarios requires considering a wider range of policy orientations and development goals. Moreover, the choice of driving factors was not exhaustive, which may have restricted our capacity to thoroughly investigate the underlying reasons for the expansion of LULC types. Hence, it is imperative for future studies to expand the scope of driving forces to attain simulations that are more scientific and precise.

4.3. Shortcomings and Prospects

While this study provides valuable insights into WY in the context of urbanization and land use changes, one notable limitation is that it does not incorporate the runoff process. As urban expansion increases, impervious surfaces lead to higher runoff, thus reducing the capacity for water conservation in urban areas. This contrasts with WY, which may be high in these areas, but their water conservation capacity is relatively poor. As such, a more holistic approach, which includes runoff and considers water conservation (derived from precipitation, evapotranspiration, and runoff), would provide a clearer picture of the overall impacts of land use changes, especially in urban environments.

In future studies, we aim to integrate the runoff process into our analysis, providing a more comprehensive understanding of how land use changes influence both WY and water conservation. This approach will allow for more accurate predictions of water resource availability, flood risks, and ecosystem services, especially in rapidly urbanizing regions.

5. Conclusions

This study leveraged the PLUS and InVEST models to evaluate spatiotemporal variations in WY in the TLB under multiple future scenarios, analyzing changes from 2000 to 2030. Between 2000 and 2020, rapid urbanization in the TLB led to the significant expansion of construction land, which in turn increased the proportion of impervious surfaces, thus contributing to an increase in WY. In humid regions like the TLB, the impact of urbanization on WY is particularly pronounced, especially in basins that were previously covered by forests or wetlands. By 2030, all scenarios examined showed an increase in WY, with the UD scenario exhibiting the most significant growth. However, the increase in WY was significantly mitigated under the EP scenario, suggesting that the strict implementation of ecological protection policies, such as the designation of ecological red lines and returning cropland to forests, can help enhance ecosystem services. Therefore, it is essential to scientifically control the scale and pace of urbanization, promoting urban green space and safeguarding ecological spaces to enhance the water conservation capacity. These efforts are crucial for reducing the risk of floods and enhancing urban resilience.

Author Contributions: Conceptualization, Y.Z. and W.Z.; Formal analysis, R.Z.; Data curation, L.L.; Writing—original draft, R.Z.; Writing—review & editing, Y.Z., W.Z., L.F. and L.L.; Supervision, Y.Z. and L.F.; Funding acquisition, Y.Z. and W.Z. All authors have read and agreed to the published version of the manuscript.

Funding: This research was funded by the National Key Research and Development Program of China under Grant No. 2022YFE0113900, the Third Xinjiang Scientific Expedition Program under Grant No. 2021xjkk1305, the National Natural Science Foundation of China under Grant No. 42071316, and Key Laboratory of Land Satellite Remote Sensing Application, Ministry of Natural Resources of the People's Republic of China under Grant No. KLSMNR-G202310.

Data Availability Statement: The original contributions presented in this study are included in the article. Further inquiries can be directed to the corresponding authors.

Acknowledgments: We thank the anonymous reviewers for their insights and constructive comments to help improve the paper.

Conflicts of Interest: The authors declare that they have no known competing financial interests or personal relationships that could have appeared to influence the work reported in this paper.

References

1. Howarth, R.B.; Farber, S. Accounting for the value of ecosystem services. *Ecol. Econ.* **2002**, *41*, 421–429. [CrossRef]
2. Sagoff, M. On the economic value of ecosystem services. *Environ. Values* **2008**, *17*, 239–257. [CrossRef]

3. Bastian, O.; Grunewald, K.; Syrbe, R.-U. Space and time aspects of ecosystem services, using the example of the EU Water Framework Directive. *Int. J. Biodivers. Sci. Ecosyst. Serv. Manag.* **2012**, *8*, 5–16. [CrossRef]
4. Chen, X.; Lin, S.; Tian, J.; Wang, Y.; Ye, Y.; Dong, S.; Gong, X.; Lin, Q.; Zhu, L. Simulation study on water yield service flow based on the InVEST-Geoda-Gephi network: A case study on Wuyi Mountains, China. *Ecol. Indic.* **2024**, *159*, 111694. [CrossRef]
5. Liu, J.; Qin, K.; Xie, G.; Xiao, Y.; Huang, M.; Gan, S. Is the 'water tower'reassuring? Viewing water security of Qinghai-Tibet Plateau from the perspective of ecosystem services 'supply-flow-demand'. *Environ. Res. Lett.* **2022**, *17*, 094043. [CrossRef]
6. Zhout, Y.; Wang, B.; Zhu, W.; Feng, L.; He, Q.; Zhang, X.; Wu, T.; Yan, N. Spatial-temporal constraints for surface soil moisture mapping using Sentinel-1 and Sentinel-2 data over agricultural regions. *Comput. Electron. Agric.* **2024**, *219*, 108835.
7. Costanza, R.; d'Arge, R.; De Groot, R.; Farber, S.; Grasso, M.; Hannon, B.; Limburg, K.; Naeem, S.; O'neill, R.V.; Paruelo, J. The value of the world's ecosystem services and natural capital. *Nature* **1997**, *387*, 253–260. [CrossRef]
8. Xie, G.-d.; Zhen, L.; Lu, C.-x.; Xiao, Y.; Chen, C. Expert knowledge based valuation method of ecosystem services in China. *J. Nat. Resour.* **2008**, *23*, 911–919.
9. Bagstad, K.J.; Semmens, D.J.; Winthrop, R. Comparing approaches to spatially explicit ecosystem service modeling: A case study from the San Pedro River, Arizona. *Ecosyst. Serv.* **2013**, *5*, 40–50. [CrossRef]
10. Peh, K.S.-H.; Balmford, A.; Bradbury, R.B.; Brown, C.; Butchart, S.H.; Hughes, F.M.; Stattersfield, A.; Thomas, D.H.; Walpole, M.; Bayliss, J. TESSA: A toolkit for rapid assessment of ecosystem services at sites of biodiversity conservation importance. *Ecosyst. Serv.* **2013**, *5*, 51–57. [CrossRef]
11. Zhang, Z.; Zhang, H.; Feng, J.; Wang, Y.; Liu, K. Evaluation of social values for ecosystem services in urban riverfront space based on the solves model: A case study of the fenghe river, Xi'an, China. *Int. J. Environ. Res. Public Health* **2021**, *18*, 2765. [CrossRef] [PubMed]
12. Waage, S. New business decision-making aids in an era of complexity, scrutiny, and uncertainty: Tools for identifying, assessing, and valuing ecosystem services. In *Handbook on the Economics of Ecosystem Services and Biodiversity*; Edward Elgar Publishing: Cheltenham, UK, 2014; pp. 546–566.
13. Li, S.; Zhou, Y.; Yue, D.; Guo, Z.; Li, Z. Scenario Simulation of Ecosystem Services Based on Land Use/Land Cover Change in the Bailong River Basin, in China. *Land* **2024**, *14*, 25. [CrossRef]
14. Huang, C.-H.; Yang, J.; Zhang, W.-J. Development of ecosystem services evaluation models: Research progress. *Chin. J. Ecol.* **2013**, *32*, 3360.
15. Smithers, J.; Gray, R.; Johnson, S.; Still, D. Modelling and water yield assessment of Lake Sibhayi. *Water SA* **2017**, *43*, 480–491. [CrossRef]
16. Ai, J.; Sun, X.; Feng, L.; Li, Y.; Zhu, X. Analyzing the spatial patterns and drivers of ecosystem services in rapidly urbanizing Taihu Lake Basin of China. *Front. Earth Sci.* **2015**, *9*, 531–545. [CrossRef]
17. Bai, Y.; Chen, Y.; Alatalo, J.M.; Yang, Z.; Jiang, B. Scale effects on the relationships between land characteristics and ecosystem services-a case study in Taihu Lake Basin, China. *Sci. Total Environ.* **2020**, *716*, 137083. [CrossRef] [PubMed]
18. López-Moreno, J.I.; Vicente-Serrano, S.; Moran-Tejeda, E.; Zabalza, J.; Lorenzo-Lacruz, J.; García-Ruiz, J. Impact of climate evolution and land use changes on water yield in the Ebro basin. *Hydrol. Earth Syst. Sci.* **2011**, *15*, 311–322. [CrossRef]
19. Nahib, I.; Ambarwulan, W.; Rahadiati, A.; Munajati, S.L.; Prihanto, Y.; Suryanta, J.; Turmudi, T.; Nuswantoro, A.C. Assessment of the impacts of climate and LULC changes on the water yield in the Citarum River Basin, West Java Province, Indonesia. *Sustainability* **2021**, *13*, 3919. [CrossRef]
20. Zhang, L.; Cheng, L.; Chiew, F.; Fu, B. Understanding the impacts of climate and landuse change on water yield. *Curr. Opin. Environ. Sustain.* **2018**, *33*, 167–174. [CrossRef]
21. Zhou, Y.; Zhu, W.; Feng, L.; Gao, J.; Chen, Y.; Zhang, X.; Luo, J. Hierarchical classification for improving parcel-scale crop mapping using time-series Sentinel-1 data. *J. Environ. Manag.* **2024**, *369*, 122251.
22. Sang, L.; Zhang, C.; Yang, J.; Zhu, D.; Yun, W. Simulation of land use spatial pattern of towns and villages based on CA-Markov model. *Math. Comput. Model.* **2011**, *54*, 938–943. [CrossRef]
23. Yuan, M.; Liu, Y.; He, J.; Liu, D. Regional land-use allocation using a coupled MAS and GA model: From local simulation to global optimization, a case study in Caidian District, Wuhan, China. *Cartogr. Geogr. Inf. Sci.* **2014**, *41*, 363–378. [CrossRef]
24. Guo, H.W.; Sun, X.Y.; Lian, L.S.; Zhang, D.; Xu, Y. Response of water yield function of ecosystem to land use change in Nansi Lake Basin based on CLUE-S model and InVEST model. *J. Appl. Ecol.* **2016**, *27*, 2899–2906.
25. Peng, K.; Jiang, W.; Deng, Y.; Liu, Y.; Wu, Z.; Chen, Z. Simulating wetland changes under different scenarios based on integrating the random forest and CLUE-S models: A case study of Wuhan Urban Agglomeration. *Ecol. Indic.* **2020**, *117*, 106671. [CrossRef]
26. Liu, X.; Liang, X.; Li, X.; Xu, X.; Ou, J.; Chen, Y.; Li, S.; Wang, S.; Pei, F. A future land use simulation model (FLUS) for simulating multiple land use scenarios by coupling human and natural effects. *Landsc. Urban Plan.* **2017**, *168*, 94–116. [CrossRef]
27. Zhang, Y.; Yu, P.; Tian, Y.; Chen, H.; Chen, Y. Exploring the impact of integrated spatial function zones on land use dynamics and ecosystem services tradeoffs based on a future land use simulation (FLUS) model. *Ecol. Indic.* **2023**, *150*, 110246. [CrossRef]

28. Tobias, J.A.; Durant, S.M.; Pettorelli, N. Improving predictions of climate change–land use change interactions. *Trends Ecol. Evol.* **2021**, *36*, 29–38.
29. Liang, X.; Guan, Q.; Clarke, K.C.; Liu, S.; Wang, B.; Yao, Y. Understanding the drivers of sustainable land expansion using a patch-generating land use simulation (PLUS) model: A case study in Wuhan, China. *Comput. Environ. Urban Syst.* **2021**, *85*, 101569. [CrossRef]
30. Wei, Q.; Abudureheman, M.; Halike, A.; Yao, K.; Yao, L.; Tang, H.; Tuheti, B. Temporal and spatial variation analysis of habitat quality on the PLUS-InVEST model for Ebinur Lake Basin, China. *Ecol. Indic.* **2022**, *145*, 109632. [CrossRef]
31. Sun, X.-X.; Xue, J.-H.; Dong, L.-N. Spatiotemporal change and prediction of carbon storage in Nanjing ecosystem based on PLUS model and InVEST model. *J. Ecol. Rural Environ.* **2023**, *39*, 41–51.
32. Wang, C.; Li, T.; Guo, X.; Xia, L.; Lu, C.; Wang, C. Plus-InVEST Study of the Chengdu-Chongqing urban agglomeration's land-use change and carbon storage. *Land* **2022**, *11*, 1617. [CrossRef]
33. Hu, N.; Xu, D.; Zou, N.; Fan, S.; Wang, P.; Li, Y. Multi-scenario simulations of land use and habitat quality based on a PLUS-InVEST model: A case study of baoding, China. *Sustainability* **2022**, *15*, 557. [CrossRef]
34. Chen, J.; Alimujiang, K.; Rukeya, R.; Bohao, W.; Fuqiang, H.; Yan, Z. Temporal and spatial variation and prediction of water yield and water conservation in the Bosten Lake Basin based on the PLUS-InVEST model. *J. Arid Land* **2024**, *16*, 852–875. [CrossRef]
35. Xu, L.; Chen, S.S.; Xu, Y.; Li, G.; Su, W. Impacts of land-use change on habitat quality during 1985–2015 in the Taihu Lake Basin. *Sustainability* **2019**, *11*, 3513. [CrossRef]
36. Taihu Basin Authority (TBA), Ministry of Water Resources (MWR). *Comprehensive Plan of the Taihu Lake Basin 2012–2030*; Taihu Basin Authority (TBA), Ministry of Water Resources (MWR): Shanghai, China, 2012.
37. Li, P.; Li, H.; Yang, G.; Zhang, Q.; Diao, Y. Assessing the hydrologic impacts of land use change in the Taihu Lake Basin of China from 1985 to 2010. *Water* **2018**, *10*, 1512. [CrossRef]
38. Shen, J.; Yuan, H.; Liu, E.; Wang, J.; Wang, Y. Spatial distribution and stratigraphic characteristics of surface sediments in Taihu Lake, China. *Chin. Sci. Bull.* **2011**, *56*, 179–187. [CrossRef]
39. Sun, X.; Xiong, S.; Zhu, X.; Zhu, X.; Li, Y.; Li, B.L. A new indices system for evaluating ecological-economic-social performances of wetland restorations and its application to Taihu Lake Basin, China. *Ecol. Model.* **2015**, *295*, 216–226. [CrossRef]
40. Verberg, K.; Stockmann, U.; Cocks, B.; Manning, B.; Austin, J. Soil water-methods to predict plant available water capacity (PAWC) using soil-landscape associations. *Grains Res. Update* **2018**, *32*, 33–43.
41. Choudhury, B. Evaluation of an empirical equation for annual evaporation using field observations and results from a biophysical model. *J. Hydrol.* **1999**, *216*, 99–110. [CrossRef]
42. Sharp, R.; Douglass, J.; Wolny, S.; Arkema, K.; Bernhardt, J.; Bierbower, W.; Chaumont, N.; Denu, D.; Fisher, D.; Glowinski, K. InVEST 3.14.1. User's Guide. *Nat. Cap. Proj.* **2020**.
43. Posner, S.; Verutes, G.; Koh, I.; Denu, D.; Ricketts, T. Global use of ecosystem service models. *Ecosyst. Serv.* **2016**, *17*, 131–141. [CrossRef]
44. Zhang, L.; Hickel, K.; Dawes, W.; Chiew, F.H.; Western, A.; Briggs, P. A rational function approach for estimating mean annual evapotranspiration. *Water Resour. Res.* **2004**, *40*, 89–97. [CrossRef]
45. Xu, X.; Liu, J.; Tan, Y.; Yang, G. Quantifying and optimizing agroecosystem services in China's Taihu Lake Basin. *J. Environ. Manag.* **2021**, *277*, 111440. [CrossRef]
46. Ocloo, D.M. Water yield of the Volta Basin under future land use and climate change. *Environ. Dev. Sustain.* **2023**, 1–26. [CrossRef]
47. Chen, X.; Wang, Y.; Cai, Z.; Wu, C.; Ye, C. Effects of land-use and land-cover change on nitrogen transport in northern Taihu Basin, China during 1990–2017. *Sustainability* **2020**, *12*, 3895. [CrossRef]
48. Samal, D.R.; Gedam, S. Assessing the impacts of land use and land cover change on water resources in the Upper Bhima river basin, India. *Environ. Chall.* **2021**, *5*, 100251. [CrossRef]
49. Yang, J.; Xie, B.; Zhang, D.; Tao, W. Climate and land use change impacts on water yield ecosystem service in the Yellow River Basin, China. *Environ. Earth Sci.* **2021**, *80*, 72. [CrossRef]
50. Yang, X.; Gu, X.; Zhang, P.; Liu, J.; Zhang, W.; Long, A. Assessment of the Impacts of Climate and Land Use Changes on Water Yield in the Ebinur Lake Basin. *Land* **2024**, *13*, 1324. [CrossRef]
51. Lang, Y.; Song, W.; Zhang, Y. Responses of the water-yield ecosystem service to climate and land use change in Sancha River Basin, China. *Phys. Chem. Earth Parts A/B/C* **2017**, *101*, 102–111. [CrossRef]
52. Canqiang, Z.; Wenhua, L.; Biao, Z.; Moucheng, L. Water yield of Xitiaoxi river basin based on InVEST modeling. *J. Resour. Ecol.* **2012**, *3*, 50–54. [CrossRef]
53. Dai, Y.; Qiao, X.; Yang, Y.; Liu, L.; Chen, Y.; Zhang, J.; Zhao, T. Optimizing Land Use to Mitigate Ecosystem Service Trade-Offs Using Multi-Scenario Simulation in the Luo River Basin. *Land* **2024**, *13*, 1243. [CrossRef]
54. Wang, P.; Wang, J.; Zhang, J.; Ma, X.; Zhou, L.; Sun, Y. Spatial-temporal changes in ecosystem services and social-ecological drivers in a typical coastal tourism city: A case study of Sanya, China. *Ecol. Indic.* **2022**, *145*, 109607. [CrossRef]

55. Tao, Y.; Li, Z.; Sun, X.; Qiu, J.; Pueppke, S.G.; Ou, W.; Guo, J.; Tao, Q.; Wang, F. Supply and demand dynamics of hydrologic ecosystem services in the rapidly urbanizing Taihu Lake Basin of China. *Appl. Geogr.* **2023**, *151*, 102853. [CrossRef]
56. Shirmohammadi, B.; Malekian, A.; Salajegheh, A.; Taheri, B.; Azarnivand, H.; Malek, Z.; Verburg, P.H. Impacts of future climate and land use change on water yield in a semiarid basin in Iran. *Land Degrad. Dev.* **2020**, *31*, 1252–1264. [CrossRef]
57. Li, Y.; Li, J.; Chu, J. Research on land-use evolution and ecosystem services value response in mountainous counties based on the SD-PLUS model. *Ecol. Evol.* **2022**, *12*, e9431. [CrossRef] [PubMed]

Disclaimer/Publisher's Note: The statements, opinions and data contained in all publications are solely those of the individual author(s) and contributor(s) and not of MDPI and/or the editor(s). MDPI and/or the editor(s) disclaim responsibility for any injury to people or property resulting from any ideas, methods, instructions or products referred to in the content.